Rheo-optical studies on the deformation mechanism of semi-crystalline polymers. IX. Dynamic birefringence behaviour of a high-density polyethylene film having row nucleated crystalline texture of *c*-axis orientation*

Thein Kyu, Naoshi Yasuda†, Shoji Suehiro‡, Takeji Hashimoto, and Hiromichi Kawai§
Department of Polymer Chemistry, Faculty of Engineering, Kyoto University, Kyoto 606, Japan
(Received 24 July 1979; revised 15 October 1980)

The dynamic birefringence behaviour of a high-density polyethylene film having a row-nucleated crystalline texture of cylindrites oriented along the machine direction of fabrication was investigated over frequency and temperature ranges covering the α mechanical dispersion of this material. The results are discussed in combination with the dynamic X-ray diffraction behaviour of the material so as to explore the structural origins of the α mechanical dispersion, not only for this particular material, but also for bulk-crystallized polyethylene having a spherulitic texture. Two deformation processes contribute to the α_1 mechanism, corresponding to the lower temperature relaxation process in the α mechanical dispersion; i.e. (i) a lamellar detwisting process involving the rotation of crystal grains within the crystal lamellae or of lamellar segments around the crystal *b*-axis or the lamellar axis, which predominates in the *MD* (machine direction) specimen, and (ii) lamellar shearing associated with the rotation of the crystal grains or the lamellar segments around the crystal *a*-axis, which is accentuated in the *TD* (transverse direction to fabrication) specimen. An additional deformation process, lamellar bending, is also observed in the *MD* specimen as being likely elastic in the dynamic response, and its contribution is found to be substantial, not to the α dispersion, but rather to the β dispersion of this material. The α_2 mechanism corresponding to the higher temperature relaxation process in the α mechanical dispersion is observed to be more pronounced in the *TD* than in the *MD* specimen. The apparent dynamic crystal lattice compliance shows a definite dispersion during activation of the α_2 mechanism, but a slight dispersion during activation the α_1 mechanism, suggesting that the α_2 mechanism must be related to an intracrystal relaxation process whereas the α_1 mechanism must be associated with an intercrystal relaxation process at their boundaries.

INTRODUCTION

In the previous papers of this series[1,2], the deformation processes underlying the α mechanical dispersion of an isotropic melt-crystallized low-density polyethylene were interpreted in terms of reorientations of lamellar segments or crystal grains involving their preferential rotations around the crystal *a*- and *b*-axes, respectively, within orienting lamellae at the polar and equatorial zones of uniaxially deformed spherulite. The specimens hitherto employed in the rheo-optical studies[1-6] were the isotropic melt-crystallized ones which possess the spherulitic crystalline texture. The local strain at the equatorial zone of uniaxially deformed spherulite is usually larger than that at the polar zone[7], reflecting from crystalline morphology of lamellar aggregation in the spherulitic texture. The time dependent deformation behaviour is also different locally with respect to the angular position of the spherulite[8]. The rheo-optical responses available from these spherulitic specimens, such as optical absorption and emission dichroism, are usually averaged over all the azimuthal angles of the spherulite, thus leading to difficulties in resolving the optical responses into fundamental structural responses, if any, unless models of spherulite deformation are postulated.

The polyethylene spherulite is composed of crystal lamellae which have grown radially, with the crystal *b*-axis parallel to the axis of growth (lamellar axis) around which the crystal *a*- and *c*-axes rotate periodically to result in the so-called lamellar twisting. Under tensile deformation of a spherulitic film of polyethylene, the crystal lamellae at the polar and equatorial zones of uniaxially deformed spherulites are parallel and perpendicular to the principal stress. Preferential rotations of the lamellar segments or crystal grains around the crystal *a*- and *b*-axes have been proposed, respectively, as the fundamental structural responses at the polar and equatorial zones of spherulite in association with the lamellar shearing and detwisting[9-16]

* Presented in part at the ACS San Francisco Meeting, August, 1976, and in part at the 26th IUPAC Congress, Tokyo, September, 1977.
† Present address: Research Center, Japan Synthetic Rubber Co. Ltd., 7569 Ikuta, Tama-ku, Kawasaki 214, Japan.
‡ Present address: Polymer Research Institute, University of Massachusetts, Amherst, Mass. 01003, U.S.A.
§ To whom correspondence should be addressed.

0032-3861/80/101205-12$02.00

The idea that is developed for overcoming the obscurity in resolving the optical responses from the spherulitic system, is to use a particular film specimen crystallized from stress-melts of polyethylene which has a row-nucleated crystalline texture grown in cylindrical symmetry along the machine direction (MD) of fabricating the film specimen[17]. The specimen has cylindrites in which stacked crystal lamellae are oriented radially with their lamellar axes highly perpendicular to the machine direction. Therefore, the structural responses that occur for tensile deformation of the specimen along the machine direction may represent those expected at the equatorial zone of spherulitic texture, whereas the responses that occur for tensile deformation of the specimen along the transverse direction (*TD*) to the fabrication may reflect the responses expected at the polar zone of the spherulitic texture.

In this paper, the dynamic mechanical and optical (birefringence) behaviour of a film specimen crystallized from the stress-melts of an extra-high molecular weight polyethylene possessing the row-nucleated crystalline texture of *c*-axis orientation will be investigated. The dynamic birefringence behaviour is discussed in conjunction with the dynamic crystal orientation and lattice deformation behaviour obtained from the dynamic X-ray diffraction studies of the same material[18] in order to explore the structural origins of the α mechanical dispersion of the row-nucleated specimen as well as isotropic melt-crystallized specimen of spherulitic texture. Discussion will be extended to the 'hard-elasticity' which is often found for the row-nucleated systems having the lamellar morphology oriented perpendicular to the machine direction of fabrication.

EXPERIMENTAL

Test specimen

An extra-high molecular weight linear polyethylene (Sholex Super 5551H, Japan Olefin Chemical Ind., Ltd) having a weight-average molecular weight of 350 000 was fed into a bumbery mixer where the pellets were melted for several minutes. The melt kept at ~ 160°C at the exit of the mixer was fed into mixing rolls controlled at 150°C and then calendered into sheet form by passing through a set of calender rolls. The temperature and relative surface velocity of these rolls were controlled so as to crystallize the melts under sufficiently high shear stress. The calendered films thus prepared have a density of 0.951 g cm^{-3} and a volume-average crystallinity of 66.6% assuming that the densities of the crystalline and amorphous phases are 1.000 and 0.852 g cm^{-3}, respectively. The detail of the fabrication processes and the characterization of these film specimens were described elsewhere[17].

Experimental procedure

Prior to the static and dynamic experiments, the above mentioned specimens were annealed by placing them between two polished stainless steel plates at 110°C for more than 5 h in an vacuum oven in order to prevent undesirable thermal effects occuring during the experiments. For the dynamic birefringence experiment, the film specimen of ~ 200 μm thickness was cut into ribbon shape of 80 mm length and 8 mm width along the machine and transverse directions, respectively, and were designated hereafter as the *MD* and *TD* specimens. The ribbon shape specimen was mounted in a tensile dynamic deformation apparatus at an initial gauge length of 60 mm and was subjected to a static tensile strain of 3.3% to avoid buckling of the specimen during imposing a dynamic tensile strain of 0.25%. A preparatory vibration was applied for ~ 1 h at 4.3 Hz at each measurement temperature in order to assure the vibrational steady state as well as to perform a sort of mechanical conditioning of the specimen. The simultaneous measurement of dynamic mechanical and dynamic birefringence behaviour was conducted by means of a π-sector technique[19] over a frequency range from 0.008 to 4.3 Hz at various temperatures from 20 to 110°C.

RESULTS

Morphology and static deformation behaviour

According to our previous electron microscopic (*EM*) and small-angle X-ray scattering (SAXS) studies[17], the above mentioned calendered specimen possesses a crystalline texture of cylindrites in which stacks of crystal lamellae are oriented radially with their lamellar axes perpendicular to the machine direction of fabrication. These lamellae are thought to overgrow from rows of nucleating points, as proposed by Keller and Machin[20], to form a sort of lamellar network. The high degree of lamellar orientation can be noticed in the lower half of *Figure* 1 in which the appearance of two-point SAXS pattern in the meridional direction for the unstretched specimen and its change with stretching the specimen in the *MD* are shown. Upon stretching the specimen in the *MD*, the following changes in the lamellar network may be seen in the *Figure*; (a) increase of interlamellar spacing, which is associated with shifting the position ($2\theta_{max}$) of the merdional SAXS intensity maximum to a lower scattering angle; (b) increase of interlamellar void formation or lower density region as a consequence of the process (a), which is associated with increase of the SAXS intensity especially at lower angles than $2\theta_{max}$; (c) increasing degree of lamellar bending and irregular deformation of lamellae, which is associated with increase of lateral breathing of the two-point SAXS patterns. The increase in the SAXS intensity and the appearance of an equatorial streak at relatively high degree of stretching, (*Figure* 1) is related to whitening of the specimen which will be discussed later.

Another interesting property of this specimen which arises from its inherent structural anisotropy is a high degree of length recovery from relatively large elongation up to ~ 40%-elongation along the *MD*, i.e., the tensile behaviour characterized by the 'hard-elasticity'[21,22]. However, such elastic property cannot be observed when the specimen is stretched in the *TD*. It is characterized by a discrete yielding phenomenon at relatively small elongation, ~ 5%-elongation, followed by plastic deformation associated with macroscopic necking of the specimen. The degree of length recovery after the yielding is far less while the breaking elongation is much larger, reflecting a much more plastic nature of the specimen along the *TD* than along the *MD*.

Upon stretching along the *MD*, the specimen starts to whiten at ~ 10%-elongation, and whitening is completed at ~ 20%-elongation. Upon further stretching, the specimen exhibits no trace of macroscopic necking, followed by a break at ~ 75%-elongation which is far less than the breaking elongation of several hundred percent in the *TD*.

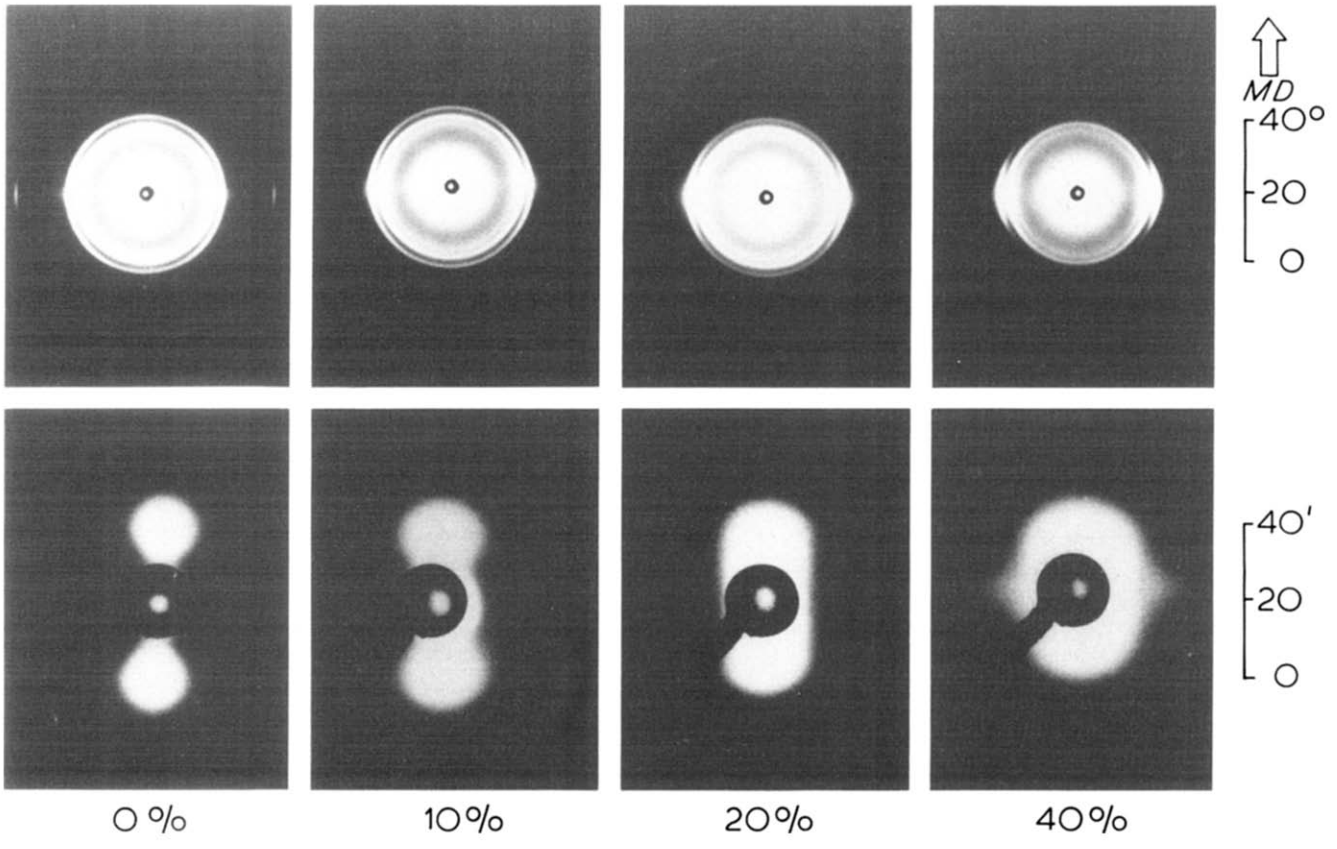

Figure 1 The changes of WAXD and SAXS patterns upon stretching the film specimen along the machine direction (*MD*); the stretching direction is vertical as indicated

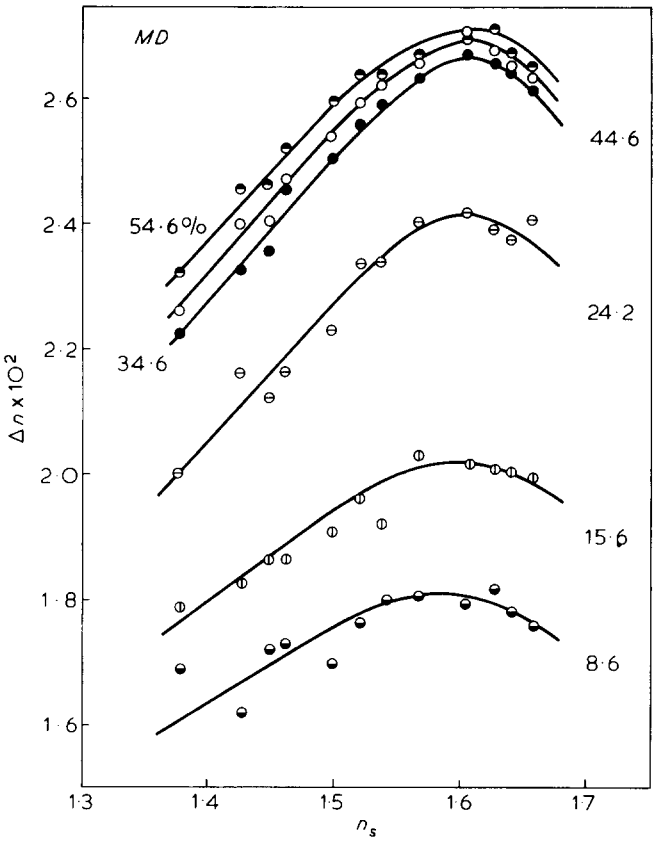

Figure 2 The change of birefringence of the film specimen with respect to the refractive indices of immersion liquids at various %-elongations along the *MD*

Upon releasing the tension, the whitening disappears almost completely unless the initial elongation exceeds 20%-elongation. The specimen also shows a marked reduction of apparent density with stretching. This behaviour of whitening and reducing in apparent density is definitely related to the development of interlamellar void or lowered density region, as mentioned above, and must contribute considerably to the dynamic birefringence measurement along the *MD*, but not along the *TD*.

Figure 2 shows the change of birefringence of the specimen with stretching along the *MD* up to ~60%-elongation and with different immersing liquids having refractive indices from 1.36 to 1.67 at room temperature. As seen in the *Figure*, the birefringence increases in positive sign with stretching and shows a maximum value at refractive index of ~1.6 of the immersing liquids. These results suggest two contributions to the birefringence; (1) resulting from orientation of some structural units having positive intrinsic birefringence towards the *MD;* (2) the negative form birefringence resulting from the generation of interlamellar void or lowered density region upon stretching.

Figure 3 shows the variation of second-order orientation factors of the three principal crystallographic axes of polyethylene crystal with %-elongation of the specimen along the *MD* at room temperature, in which the orientation factor of the *k*th crystal axis is defined as $F_k^0 = (3\langle\cos^2\theta_k\rangle - 1)/2$ with θ_k being the angle between the *k*th crystal axis and the stretching direction. In unstretched state, the orientation factor of the crystal *b*-axis F_b^0 is ~ -0.5, suggesting that the crystal *b*-axis, which coincides with the lamellar axis, orients perpendicular to

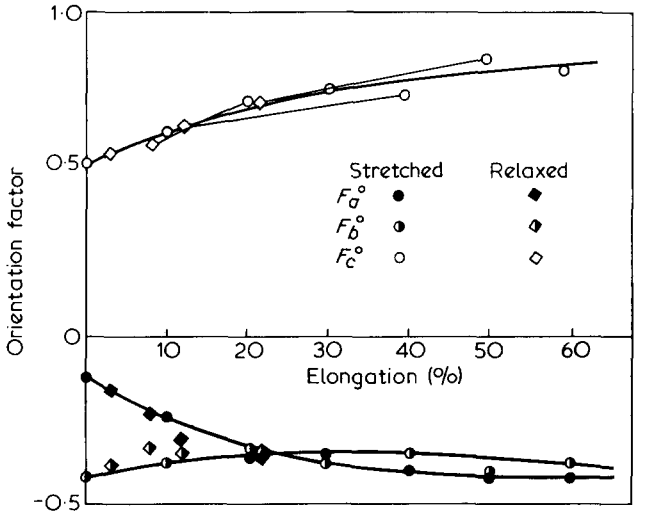

Figure 3 The changes of second-order uniaxial orientation factors of the principal crystallographic axes, F_a^0, F_b^0, and F_c^0, with %-elongation of the film specimen along the *MD*

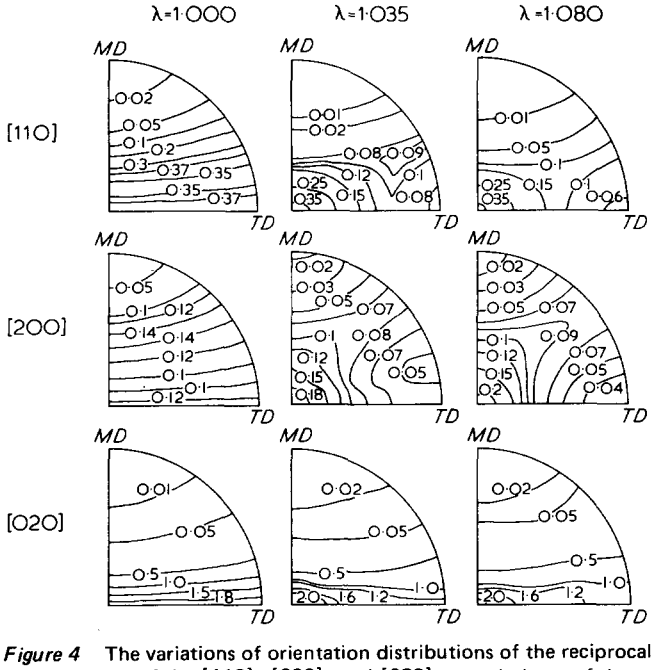

Figure 4 The variations of orientation distributions of the reciprocal lattice vectors of the [110], [200], and [020] crystal planes of the specimen, in terms of the pole figures, with 0%, 3.5%, and 8.0%-elongations along the *TD*

the *MD*. This agrees with the evidence achieved in the previous *EM* study[17] and the SAXS and WAXD results in *Figure* 1. As a consequence of preferential *c*-axis oreintation along the *MD*, the orientations of the crystal *a*- and *c*-axes are not random around the lamellar axis; i.e. $F_a^0 \neq F_c^0$ (*Figure* 3). Upon stretching, the orientation factor F_c^0 increases while F_a^0 decreases, indicating that the crystal *c*- and *a*-axes orient towards and away from the stretching direction, respectively. The F_b^0, however, changes slightly as compared to F_a^0 and F_c^0. These changes in the orientation factors should result primarily from the lamellar detwisting process involving the rotation of lamellar segments or crystal grains within the lamella around the lamellar axis or crystal *b*-axis owing to straining of interlamellar non-crystalline materials, such as tie-chain molecules between the lamellae. The minor change in F_b^0 which increases with increasing %-elongation may be attributed to a process of lamellar bending between tie-links in a fashion analogous to a leaf-spring[23]. The change of these orientation factors can be interpreted in terms of two fundamental processes; i.e. the lamellar detwisting and lamellar bending. The former process is believed to have a much greater contribution to the crystal orientation but is much slower in the dynamic response than the latter process of lamellar bending.

Figure 4 shows the variation of orientation distribution of reciprocal lattice vectors of the *k*th crystal plane with stretching the specimen along the *TD*; i.e. the changes in the pole figure of contour lines of normalized intensity distribution of X-ray diffraction from the [110], [200] and [020] crystal planes. The orientation distribution of the *k*th crystal plane in the unstretched state is cylindrical symmetry with respect ot the *MD*, (as expected from its row-nucleated crystalline texture), but not with respect to the *TD*. This invalidates the representation of the orientation behaviour with stretching along the *TD* simply in terms of the second-order orientation factor F_k^0 with respect to the *TD* alone. Upon stretching along the *TD*, the orientation distributions of the reciprocal lattice vectors of these crystal planes change in such ways that the distribution maxima accentuate in the thickness direction of the film specimen. Although the pole figure for the [020] crystal plane does not appreciably change near the polar region (the region near the *MD* in *Figure* 4), it drastically changes near the equatorial region (the region near the *TD*) to set on the crystal *b*-axis parallel to the thickness direction. However, the variation in the orientation distribution for the [200] crystal plane changes comparatively slowly with elongation ratio. Though a possible deformation mechanism may include a slight orientation of the crystal *a*-axis, intralamellar shearing involving the rotation of the crystal grains around their crystal *a*-axes, particularly in the lamellae oriented parallel to the *TD*, may be considered as a major process during stretching of the specimen in the *TD* up to the yield point.

Figure 5 shows a diagram schematizing two types of representative deformation processes during stretching of the specimen along the *MD* and *TD*, respectively; i.e. the lamellar detwisting and intralamellar shearing involving the two types of preferential rotations of crystal grains around the crystal *b*- and *a*-axes for the *MD* and *TD* specimens, respectively.

Dynamic mechanical dispersion

Temperature dependences of the real and imaginary components of complex dynamic tensile modulus func-

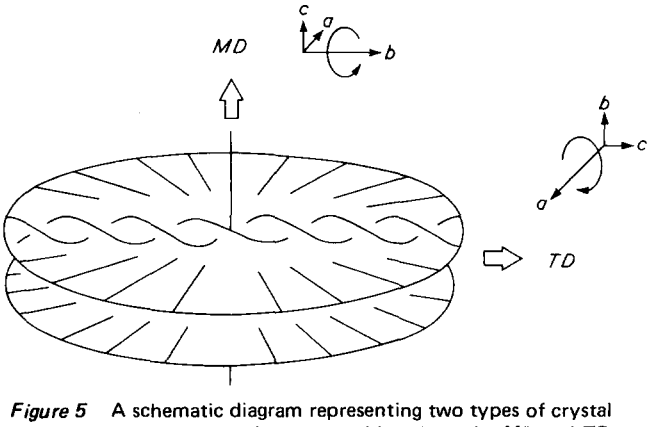

Figure 5 A schematic diagram representing two types of crystal deformation mechanisms during stretching along the *MD* and *TD*

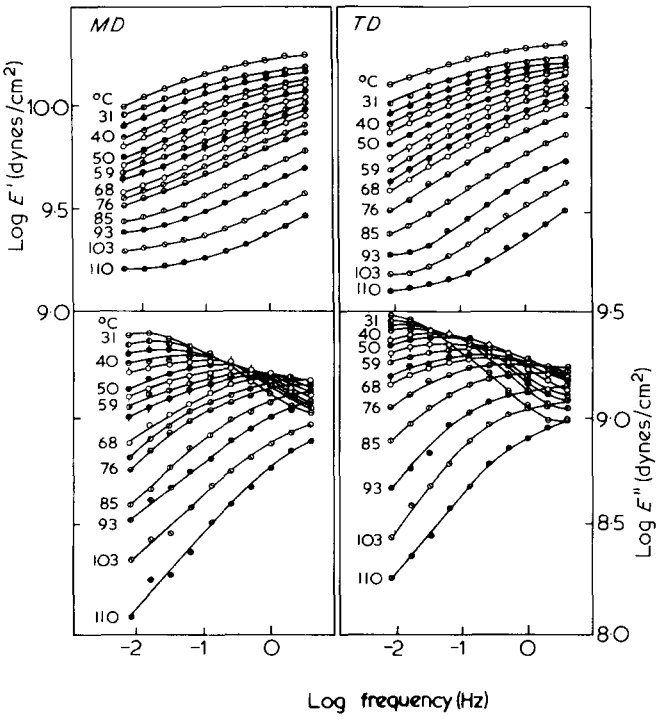

Figure 6 Temperature dependences of the storage and loss modulus functions of the *MD* and *TD* specimens

tion; i.e. the storage and loss modulus functions $E'_T(v)$ and $E''_T(v)$, for the *MD* and *TD* specimens are shown in the left- and right-hand sides of *Figure* 6. The modulus functions decrease markedly with increasing temperature (see *Figure* 6 and previous study on spherulitic low and medium density polyethylenes[6]). This decrease does not allow a conventional frequency-temperature superposition of shifting the modulus functions horizontally along the logarithmic frequency axis by a shift of $\log a_T(T,T_0)$. A considerable vertical shift of the functions by $\log b_T(T,T_0)$ is required to obtain smoothed master curves at a reference temperature of T_0, even though the master curves are only apparent from linear viscoelasticity for a system having more than one relaxation mechanism.

Therefore, the superposition was performed by a combination of vertical and horizontal shifts resulting in the apparent master curves of the storage and loss modulus functions reduced to a common reference temperature of 50°C for the *MD* and *TD* specimens, respectively (*Figures* 7 and 8). Broad mechanical dispersion is observed for both specimens. The dispersion is steeper in E' and broader in E'' for the the *TD* specimen than for the *MD* specimen. These unusually broad dispersion peaks in E'' and somewhat asymmetric shape of them with respect to the reduced logarithmic frequency, suggest that more than one relaxation mechanism is contributing to the dispersion. The relaxation intensity (the integrated area under the loss modulus curve) of the dispersion in the *TD* specimen is greater than that of the *MD* specimen.

Temperature dependence of the horizontal shift factor $a_T(T,T_0)$ is plotted in its logarithm against reciprocal absolute temperature in *Figure* 9. The Arrhenius plots can be represented by two straight lines with activation energies of relaxation processes of 25.2 and 33.6 kcal mol^{-1} for the *MD* specimen. The corresponding results observed for the *TD* specimen are also composed of two straight lines having the activation energies of 25.4 and 37.5 kcal mol^{-1}, respectively. Temperature and frequency ranges of the dynamic measurements in these experiments to cover the storage modulus values from 1×10^{10} to $1 \times 10^{9.5}$ dyne cm^{-2}, primarily correspond to the vicinity of the α mechanical dispersion of polyethylene. The activation energies for the relaxation process at the lower temperature side, found to be 25.2 and 25.4 kcal mol^{-1} for the *MD* and *TD* specimens, are consistent with the literature value of the α_1 relaxation process of polyethylene[4,24-27]. These results suggest that the low temperature process should be assigned to the α_1 mechanical dispersion, the structural origin of which will be discussed later in connection with the dynamic birefringence and dynamic X-ray diffraction data of these specimens.

The relaxation process at the higher temperature side having the activation energies of 33.6 and 37.5 kcal mol^{-1} for the *MD* and *TD* specimens, respectively, may be assigned to the α_2 relaxation process, though the values of the activation energy obtained are relatively low compared with the literature values of ~45 kcal/mol[24,28]. This discrepancy may be due to the lack of proper separation of the contribution of the α_1 process from the viscoelastic

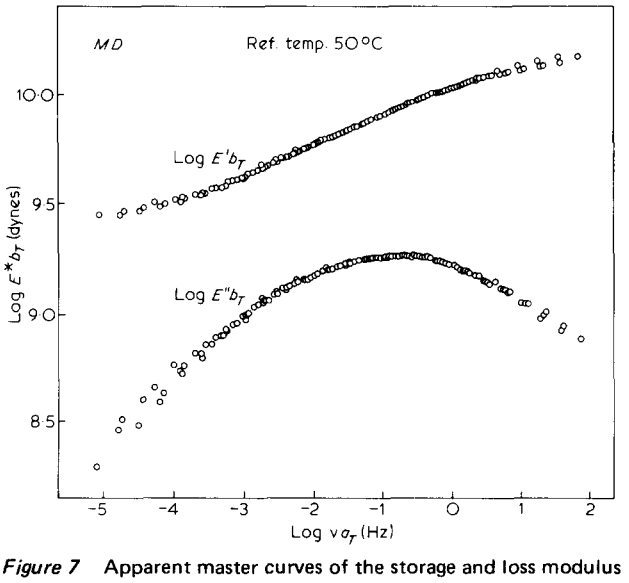

Figure 7 Apparent master curves of the storage and loss modulus functions of the *TD* specimens, reduced to a reference temperature of 50°C

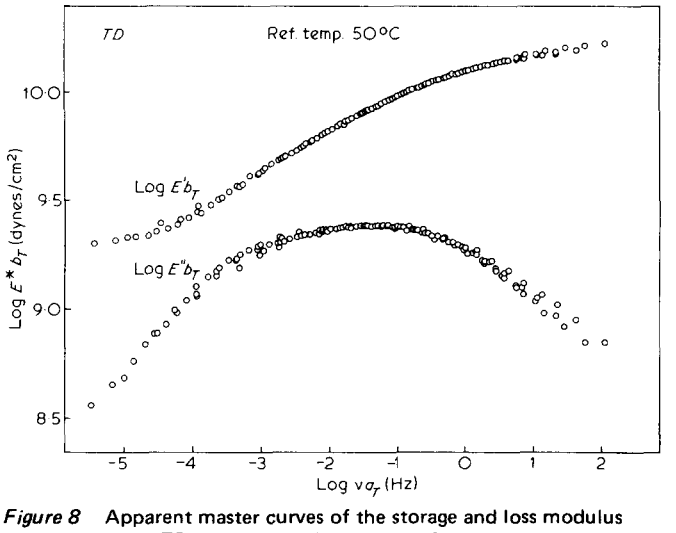

Figure 8 Apparent master curves of the storage and loss modulus functions of the *TD* specimen, reduced to a reference temperature of 50°C

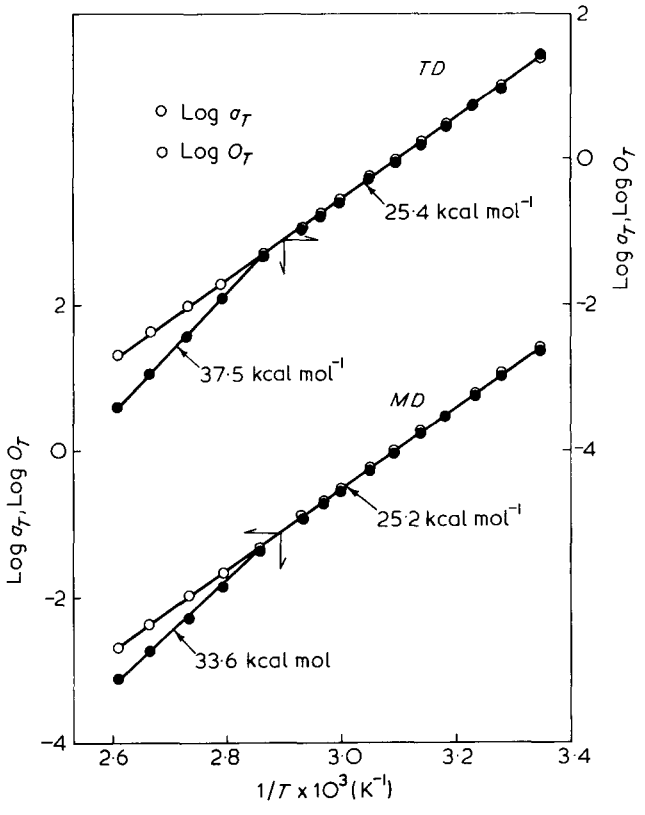

Figure 9 Arrhenius plots of the horizontal shift factors, $a_T(T,T_0)$ and $o_T(T,T_0)$, for composing the apparent mechanical and optical master curves for the *MD* and *TD* specimens

functions in the α_2 region. The temperature at which the two straight lines in the log a_T vs. $1/T$ plot intercross to each other is found at ~70°C for both specimens. This temperature corresponds to the crystal disordering temperature at which the thermal expansion coefficient of the crystal lattice spacing changes abruptly especially along the crystal *a*-axis[18]. The α_2 process has therefore, been postulated to relate to the onset of rotational vibration of chain molecules within the crystal lattice; i.e., the incoherent lattice vibration within crystals in which the intermolecular potential suffers a smearing effect to change the nature of crystal from elastic to viscoelastic[29,30]. Some related evidences will be demonstrated later in terms of the dynamic crystal lattice deformation behaviour obtained from dynamic X-ray diffraction measurements of the specimens.

The α_2 dispersion seems to be more pronounced in the *TD* specimen than in the *MD* specimen, resulting in the steeper change in E', the broader peak in E'', and, consequently, the more intensive α dispersion, as a whole, for the *TD* specimen than for the *MD* specimen, as mentioned above. This may be explained in terms of the fact that stretching along the lamellar axis (*TD* direction), which corresponds to the principal stress field direction being perpendicular to the intralamellar chain direction, can activate the α_2 process more easily than stretching along the chain direction (*MD* direction).

In *Figure* 10 are shown temperature dependences of the vertical shift factor $b_T(T,T_0)$ for the *MD* and *TD* specimens in terms of their logarithms plotted against linear scale of temperature. As can be seen in the *Figure*, the temperature dependences can be approximated by straight lines having almost identical slopes of 0.0033 and 0.0031 deg^{-1}, respectively, for the *MD* and *TD* specimens. Although the slopes are a little steeper than those for spherulitic low and medium density polyethylenes; 0.0024 and 0.0025 deg^{-1}, respectively, the temperature dependence has been fully discussed in a previous paper[6] in terms of the smearing-out effect on the intermolecular potential within the crystal lattice.

Dynamic optical dispersion

The dynamic birefringence behaviour observed simultaneously with the dynamic mechanical behaviour is analysed in terms of the in-phase and out-of-phase components of complex dynamic strain-optical coefficient function defined as being the ratio of dynamic birefringence amplitude to dynamic strain amplitude. In *Figure* 11 are shown temperature dependences of the in-phase and out-of-phase components of the strain-optical coefficient function, $K'_T(v)$ and $K''_T(v)$, for the *MD* specimen. As can be seen in the *Figure*, K' has negative values at low temperatures or at high frequencies, but increases to positive values with increasing temperature or with decreasing frequency. K'' exhibits distinct peaks at elevated temperatures and retains negative values throughout the experimental range. The peak value in $-K''$ decreases with increasing temperature, suggesting that a simple horizontal shift alone is inadequate to obtain a superposed master curve. Superposition is performed by the combination of horizontal and vertical shifts in both K' and K''. The apparent master curves of the in-phase component $(K' + p_T')$ and out-of-phase component $-(K'' - p_T'')$ of the dynamic strain-optical coefficient function reduced to a reference temperature of 50°C are shown in *Figure* 12, where the terms of p_T and o_T are the vertical and horizontal shift factors, respectively, in the superposition. The in-phase component $(K' + p_T')$ decreases from positive to negative values with increasing reduced frequency, whereas the out-of-phase component $-(K'' - p_T'')$ remains in positive value with a distinct maximum at ~-2.2 in the log reduced frequency.

The transition from positive to negative values of the in-phase component, irrespective of the out-of-phase component remaining in the same sign, suggests that the

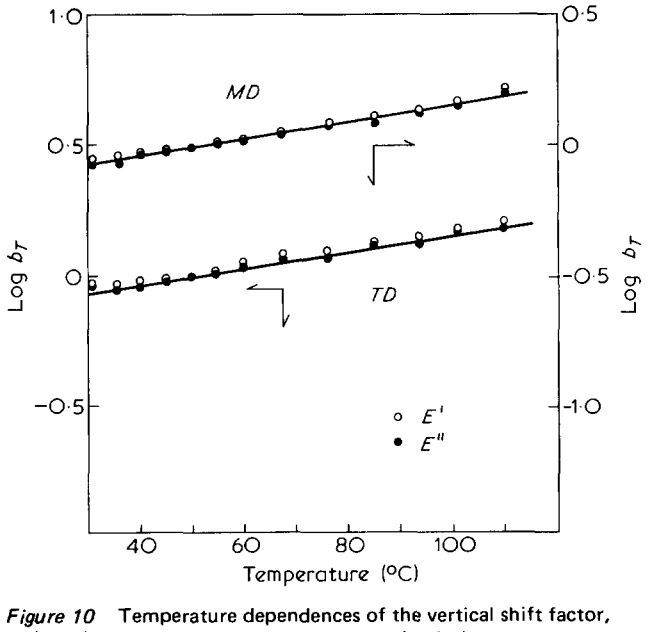

Figure 10 Temperature dependences of the vertical shift factor, $b_T(T,T_0)$, for composing the apparent mechanical master curves for the *MD* and *TD* specimens

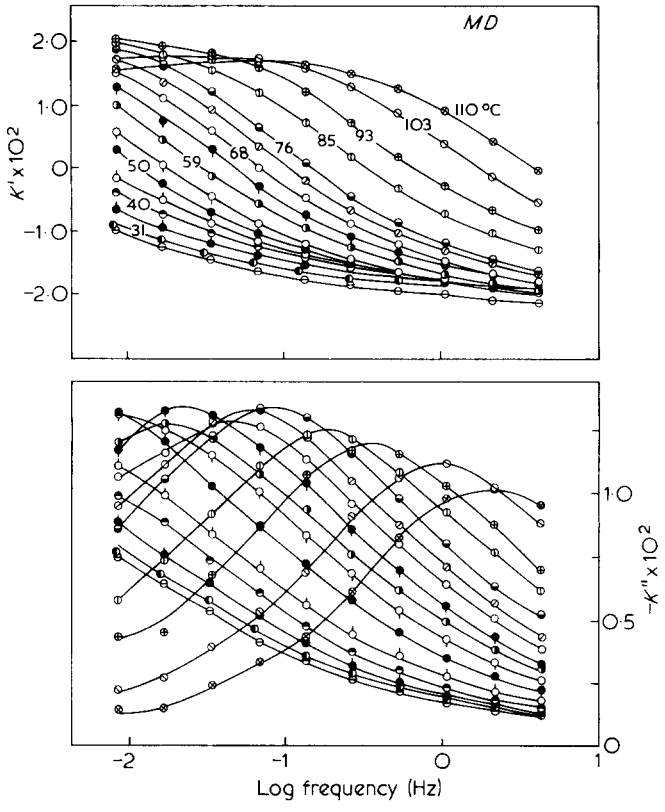

Figure 11 Temperature dependences of the in-phase and out-of-phase components of the complex dynamic strain-optical coefficient function of the *MD* specimen

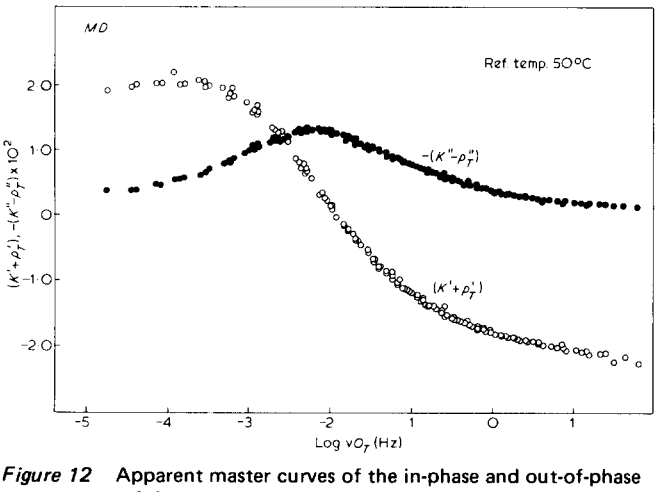

Figure 12 Apparent master curves of the in-phase and out-of-phase components of the complex dynamic strain-optical coefficient function of the *MD* specimen, reduced to a reference temperature of 50°C

dynamic birefringence changes in the phase relation from lagging to leading with respect to the dyamic bulk strain with increasing frequency. This change of the phase relation should be understood in association with the following two deformation process; namely, (i) the lamellar detwisting process which gives rise to positive birefringence due to molecular orientations, and (ii) the lamellar bending or splaying apart process which causes negative form birefringence. As shown in *Figure* 2, the splaying apart of the interlamellar spacing or lamellar bending process leading to the negative form birefringence yields a greater contribution to the dynamic birefringence than the lamellar detwisting process at low temperatures or at high frequencies. The negatively contributing lamellar bending or splaying apart process may be activated evenly throughout the experimental range, while the lamellar detwisting process is hardly activated at low temperatures or high frequencies. Consequently, the K' must be positive at low reduced frequencies in association with dominant contribution of the lamellar detwisting process, but be negative at high reduced frequencies in association with the dominant contribution of the lamellar bending or splaying apart process. The lamellar bending or splaying apart process must be quick enough in the dynamic response with almost zero contribution to the out-of-phase component. A rather broad but distinct dispersion in the out-of-phase component $-(K''-p_T'')$ must be understood as resulting primarily from the lamellar detwisting process.

Figure 13 shows master curves of the in-phase and out-of-phase components of the complex dynamic strain-orientation coefficient function of the kth crystallographic axis, $C'_{k,T_0}(\nu c_T)$ and $C''_{k,T_0}(\nu c_T)$, which were obtained from the dynamic X-ray diffraction measurements of the *MD* specimen and were reduced to a common reference temperature of 50°C[18]. As can be seen in the *Figure*, the in-phase component of the crystal b-axis C'_b does not appreciably change with the reduced frequency, whereas the C'_a and C'_c for the crystal a- and c-axes decrease markedly in their absolute values with increasing frequency. The out-of-phase component of the C''_b remains almost zero, while those of the C''_a and C''_c show distinct peaks, both corresponding to the above dispersion behaviour of the in-phase components.

These characteristic dynamic orientation behaviour of the crystallographic axes strongly suggest a dynamic orientation dispersion of the crystallites in such a particular fashion that the dynamic rotation of the crystal a-

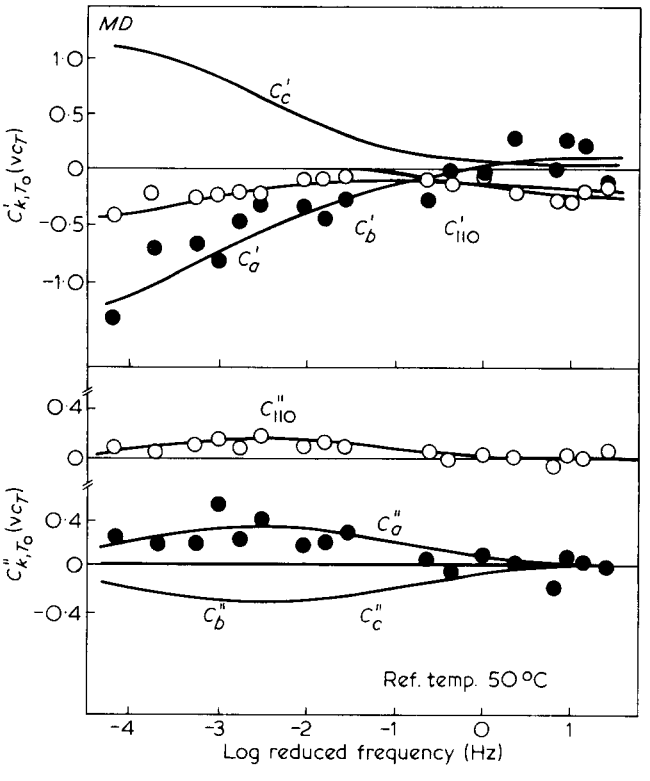

Figure 13 Master curves of the in-phase and out-of-phase components of the complex dynamic strain-orientation coefficient functions of the kth crystallographic axis for the *MD* specimen, reduced to a reference temperature of 50°C

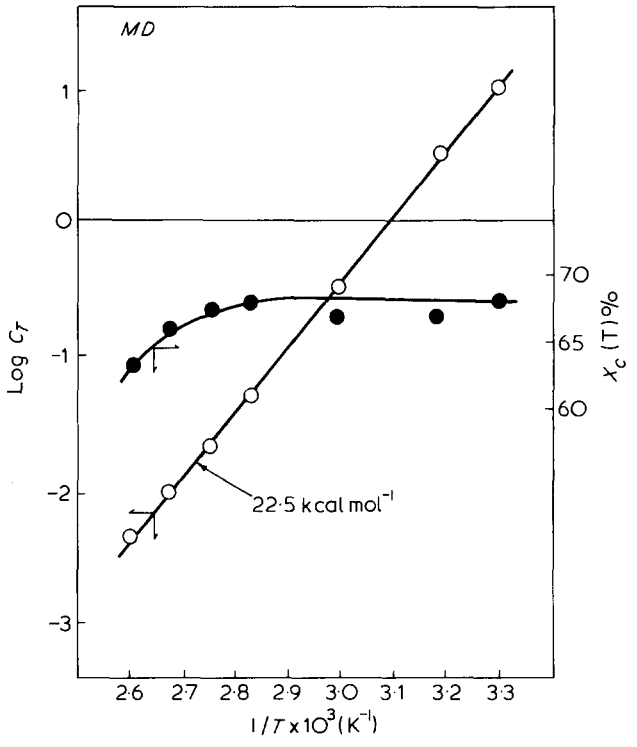

Figure 14 Arrhenius plots of the horizontal shift factors, $c_{T,k}(T,T_0)$, for composing the orientation master curves of the kth crystallographic axis for the *MD* specimen

and c-axes around the crystal b-axis. This dynamic rotation definitely corresponds to the lamellar detwisting process. The opposite sign in the in-phase and out-of-phase components implies that the dynamic crystal rotation is lagging behind the dynamic bulk strain. The dispersion peaks of the C''_a and C''_c correspond to that of the strain-optical coefficient function in *Figure* 12 appearing at the same reduced frequenices ranging from 0.001 to 0.01 Hz. The activation energy as determined from the Arrhenius plots of the temperature dependence of the horizontal shift factor $c_T(T,T_0)$ was found to be 22.5 kcal mol^{-1}, as shown in *Figure* 14. This value is in good accord with those determined from the $a_T(T,T_0)$ and $o_T(T,T_0)$ versus $1/T$ for the dynamic mechanical and optical functions, as illustrated in *Figure* 9, as well as to the literature values for the α_1 mechanical dispersion. The lamellar detwisting process is the major contribution to the α_1 mechanical dispersion for the *MD* specimen. The C''_c and $-(K''-p_T'')$ remain almost close to zero at high reduced frequencies, while the $(K'+p_T')$ shows a remarkable negative value at these high reduced frequencies. These facts suggest that the remarkable negative value should not be related to the lamellar detwisting process, but be attributed to the negative form birefringence arising from the lamellar bending process of almost non-delayed response with respect to the dynamic bulk strain.

The complementary results of the in-phase and out-of-phase components of the complex dynamic strain-optical coefficient function for the *TD* specimen are shown in *Figure* 15 as a function of temperature. The corresponding master curves reduced to the common reference temperature of 50°C after superposing the functions are shown in *Figure* 16. The reduced in-phase component $(K'+p_T')$ decreases rapidly with increasing reduced frequency, but, in contrast to the *MD* specimen, it remains positive except for a slight negative at high reduced frequencies. This slight negative value should be understood as resulting from lamellar orientation towards the *TD*, but not as from any development of the negative form birefringence. The reduced out-of-phase component $-(K''-p_T'')$ remains also positive throughout the reduced frequency range, exhibiting a distinct peak at the frequency region at which the dispersion of the in-phase component occurs. These results indicate that the dynamic birefringence lags behind the applied bulk strain with a frequency dispersion at ~ -2.5 in the reduced log frequency, a little lower than that found for the *MD* specimen.

Contrary to the orientation distributions of the crystalline structural units in the *MD* specimen, the orientation in the *TD* specimen are not cylindrical symmetry with respect to the *TD*. This leads to a difficulty of representing the dynamic orientation behaviour of the units in terms of the complex dynamic strain-orientation coefficient function C^*_k defined as the ratio of dynamic amplitude of the second-order uniaxial orientation factor ΔF_k^* to the dynamic strain amplitude $\Delta\lambda^*$. It is, however, believed that the birefringence dispersion is caused by the orientation dispersion of the crystallites in association with preferential dynamic rotation of lamellar segments or crystal grains within the lamellae around their crystal a-axes due to intralamellar shearing. These interpretations may be predicted qualitatively from *Figure* 4 in terms of

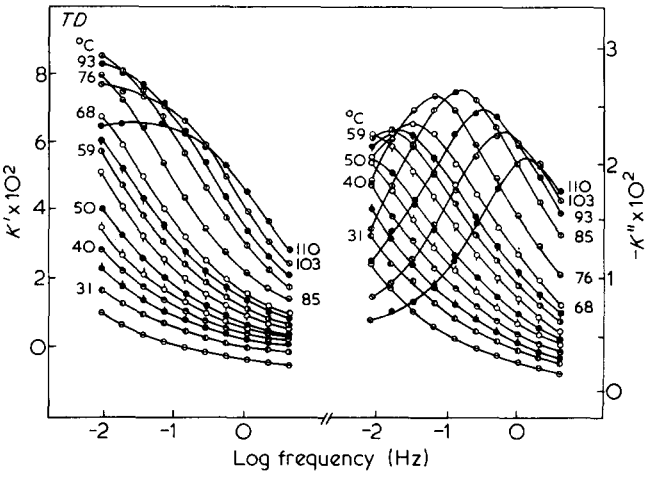

Figure 15 Temperature dependences of the in-phase and out-of-phase components of the complex dynamic strain-optical coefficient function of the *TD* specimen

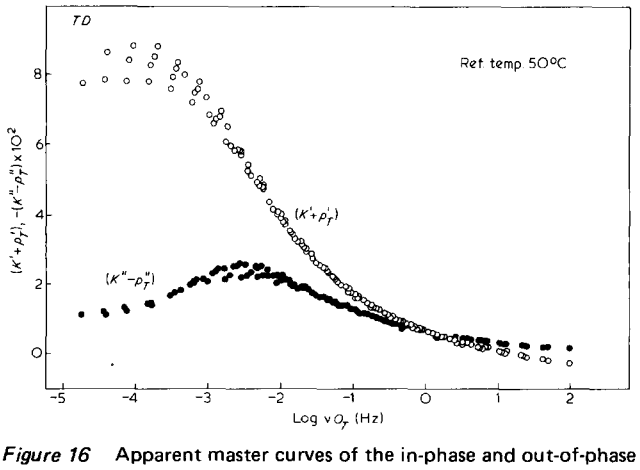

Figure 16 Apparent master curves of the in-phase and out-of-phase components of the complex dynamic strain-optical coefficient function of the *TD* specimen, reduced to a reference temperature of 50°C

the change of pole figure of the kth crystal plane with static extension ratios up to the yielding, and were demonstrated quantitatively in the previous paper[18] in terms of the dynamic behavior of the orientation distribution function of the kth crystal plane, $\Delta q_k^*(\theta_k,\varphi)$. It is again noted that the relaxation intensity of the strain-optical coefficient function (the integrated area under the master curve of $-(K''-p_T'')$) of the *TD* specimen is much greater than that of the *MD* specimen. This is consistent with that for the mechanical relaxation intensity mentioned above.

The Arrhenius plots of temperature dependence of the horizontal shift factor $o_T(T,T_0)$ are represented, in contrast to those of $a_T(T,T_0)$, by a single straight line, as seen in *Figure* 9, determining the activation energies to be 25.2 and 25.4 kcal mol^{-1}, respectively, for the *MD* and *TD* specimens. The activation energy for the *TD* specimen is also very consistent with those for the α_1 mechanical dispersion. Though the orientational birefringence may not be sensitive to the rotational vibration of chain molecules within the crystal lattice, the intrinsic birefringence of the chain molecule should be influenced by the internal field effect, if any. The reason why no prominent optical dispersion corresponding to the α_2 process is observed in the Arrhenius plots of $o_T(T,T_0)$, may be owing to the fact that the internal field effect upon the intrinsic birefringence is comparatively small as compared to the orientational birefringence at these temperatures. However, the cross-over of K' at high temperatures and low frequencies, as seen in *Figures* 11 and 15, and the feathering off of $(K'+p_T')$ at low reduced frequencies, as seen in *Figures* 12 and 16, may reflect the contribution of the α_2 process through the internal field effect. Actually, the temperature dependence of the vertical shift factors p_T' and p_T'' do change rather abruptly at the high temperatures, as can be seen in *Figure* 17.

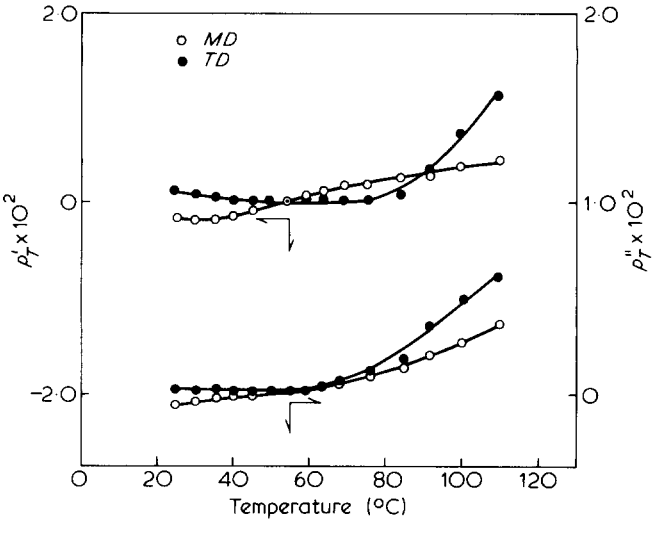

Figure 17 Temperature dependences of the vertical shift factors, p_T' and p_T'', for composing the apparent optical master curves for the *MD* and *TD* specimens

To elucidate the nature of the α_2 process, a more elaborate and direct evidence can be achieved from the measurements of dynamic crystal lattice deformation behavior by means of dynamic X-ray diffraction technique[31], i.e. the measurement of complex dynamic crystal lattice compliance J_k^*. Temperature dependences of the real and imaginary components of the crystal lattice compliance function are shown in *Figure* 18 for the [110], [200] and [020] crystal planes for the *TD* specimen[18]. The real component does not exhibit any frequency dependence and the imaginary component remains almost zero both at low temperatures. However, they begin to show frequency dependence at high temperatures cor-

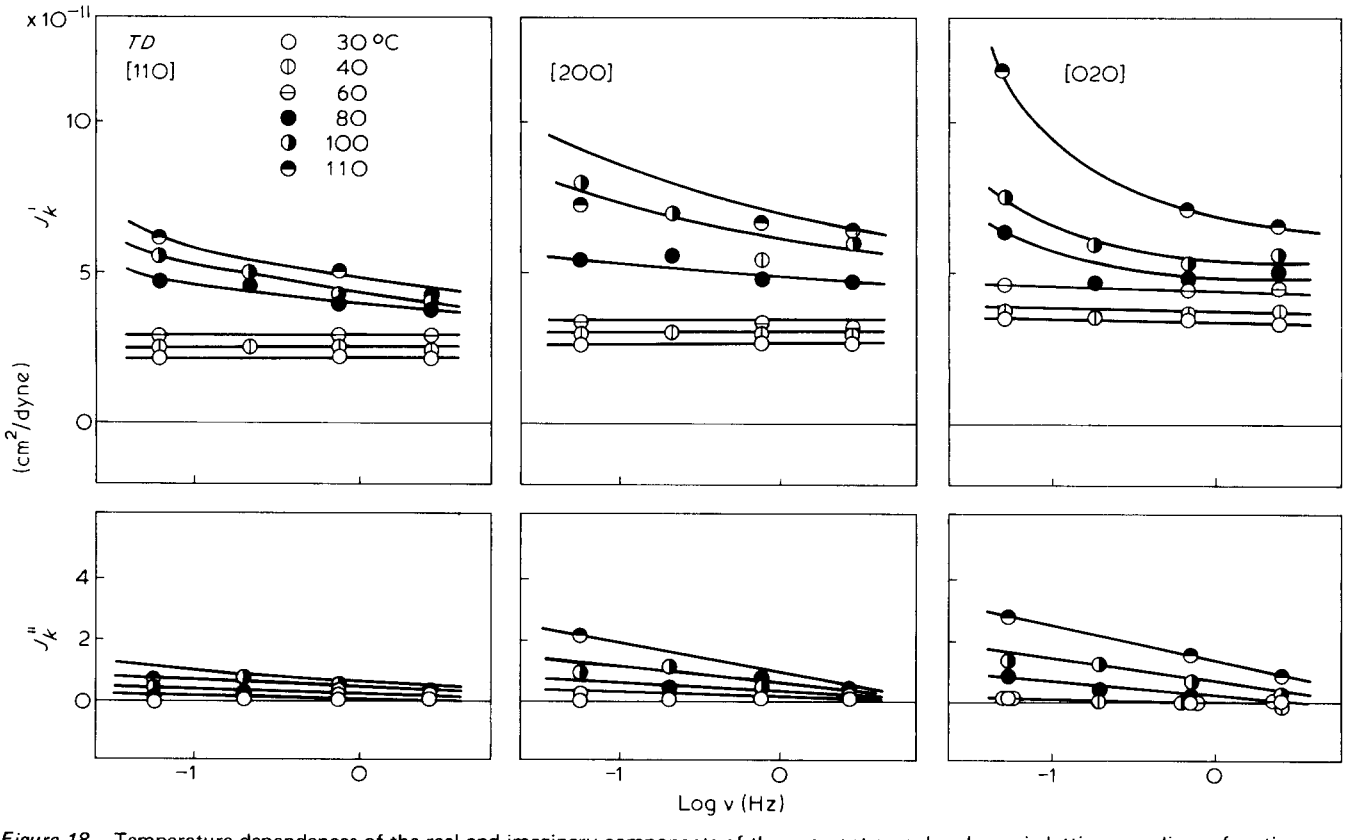

Figure 18 Temperature dependences of the real and imaginary components of the apparent complex dynamic lattice compliance functions, J_k' and J_k'', of the [110], [200], and [020] crystal planes for the *TD* specimen

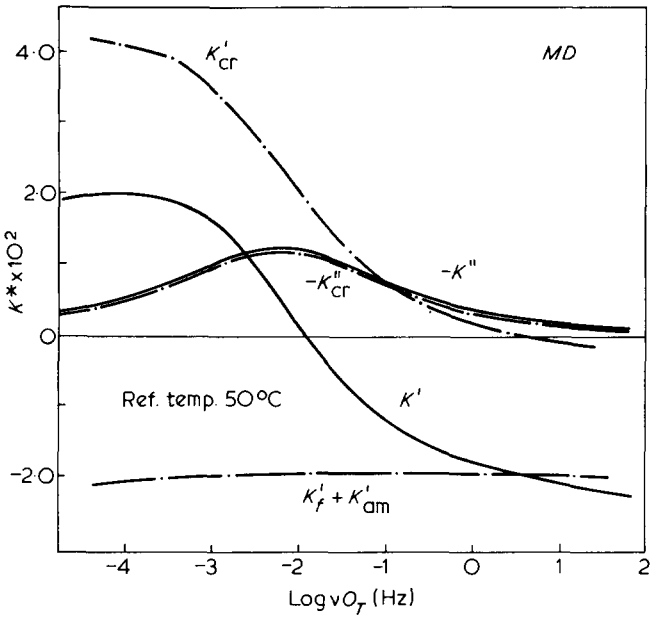

Figure 19 Separation of the optical dispersion K^* of the *MD* specimen into the contributions from crystalline, noncrystalline and form birefringences

responding to the temperature region of the α_2 process. In other words, the crystal is elastic in its response at the low temperatures, but becomes viscoelastic at the high temperatures, indicating that the α_2 process is an intracrystal relaxation phenomenon, while the α_1 process is an intercrystal grain-boundary relaxation phenomenon associated with dynamic orientation of the crystal grains.

Separation of optical dispersion into contributions of crystalline, non-crystalline and form birefringences

The optical dispersion in the *MD* specimen is attributed mainly to the lamellar detwisting process. Also an assignment for the negative form birefringence, which leads to the negative $(K' + p_T')$ at high reduced frequencies, is made to the lamellar bending or splaying apart process. All these discussions are confined to a qualitative manner, and it is uncertain either to what extent the crystalline contribution is to the optical dispersion associated with the lamellar detwisting process or whether the lamellar bending process is a time-dependent process. Therefore, let us separate the optical dispersion observed into three contributions from crystalline, non-crystalline and form birefringences on the basis of an approximation of the two-phase hypothesis of semicrystalline polymers.

The strain-optical coefficient can be expressed for a uniaxially oriented polyethylene as follows[32]:

$$K = (\delta\Delta/\delta\lambda)_{\lambda=\lambda 0} = X_c[(n_a - n_c)C_a + (n_b - n_c)C_b] + (1 - X_c)\Delta^0{}_{am}C_{am} + (\delta\Delta_f/\delta\lambda) = K_{cr} + K_{am} + K_f \quad (1)$$

where X_c is the volume fraction of crystalline phase, n_i is the principal refractive index of polyethylene crystal, C_i is the strain-orientation coefficient, and $\Delta^0{}_{am}$ is the intrinsic birefingence of noncrystalline chain segment. The subscripts, *cr*, *am*, and *f* denote the crystaline, noncrystalline and form birefingences. For the complex dynamic strain-optical coefficient function, equation (1) can be modified simply by rewriting the K and C in terms of the complex variables as follows;

$$K^*_T(iv) = X_c(T)\sum_k^{a,b}(n_k - n_c)_T C^*_{k,T}(iv) + [1 - X_c(T)]\Delta^0{}_{am,T}C^*_{am,T}(iv) + (\delta\Delta_f{}^*/\delta\lambda^*)_T = K^*_{cr,T}(iv) + K^*_{am,T}(iv) + K^*_{f,T}(iv) \quad (2)$$

The last term of equation (2) is usually assumed to be negligibly small for spherulitic crystalline specimen. However, for the *MD* specimen, the contribution of the form birefringence is substantial, as demonstrated in *Figure* 2, and cannot be ignored. Assuming the principal refractive indices of polyethylene crystal to be the same as those of *n*-paraffin; $n_a = 1.514$, $n_b = 1.519$, and $n_c = 1.575$, as determined by Bunn and Daubeny[33], and to be temperature independent, the separation of crystalline contribution from the optical dispersion according to equation (2) is conducted using $C^*_{k,T_0}(ivc_T)$ in *Figure* 13 and $X_c(T)$ in *Figure* 14. The results are shown in *Figure* 19 in terms of dash-dot lines.

Obviously, the out-of-phase component of the complex dynamic strain-optical coefficient function of the crystalline phase, K''_{cr,T_0}, is found to be quite consistent with that of the total strain-optical coefficient function, $K''_{T_0}(\nu o_T)$, hence the $(K''_{am,T_0} + K''_{f,T_0})$ must be almost zero in the reduced frequency range covered here. The K'_{cr,T_0} is determined to be considerably larger than $K'_{T_0}(\nu o_T)$, decreasing from much larger positive value to slightly negative value with increasing reduced frequency. The shape of the K'_{cr} is, however, similar to that of the K', leading to the separated $(K'_{am,T_0} + K'_{f,T_0})$ to be negative and hardly frequency dependent. These results suggest that the optical dispersion of K^* is mainly attributed to the crystalline contribution associated with the lamellar detwisting process. Now, one can conclude that the large negative values of K' at high reduced frequencies are caused by the negative contribution of $(K'_{am,T_0} + K'_{f,T_0})$. It is felt that the K'_{am} may contribute to the positive value, therefore, the negative contribution should be inherent in K'_f which is believed to be associated with the lamellar bending or splaying apart process. The reason that the frequency dependence of the $(K'_{am} + K'_f)$ is not appreciable, may be due to the fact that the lamellar bending process as well as the orientation of amorphous chains between the bending lamellae respond quite in phase with the dynamic bulk strain, at least, in this reduced frequency range. The frequency dispersion of $(K'_{am} + K'_f)$, if any, must be expected in the β dispersion region which is much higher than this reduced frequency range.

DISCUSSION

As a general and concomitant discussion, let us survey the assignments to the α mechanical dispersion of polyethylene proposed by other authors, hitherto, in comparison with those achieved by the present authors through a series of rheo-optical studies of polyethylenes bulk-crystallized from isotropic as well as stressed melts. The assignment to the α_2 dispersion corresponding to the higher temperature process of the α mechanical dispersion seems to have been established as being caused by the onset of rotational vibration of intracrystalline chain molecules to change the polymer crystal from elastic to viscoelastic material, though no direct and definite dynamic experimental evidence has yet been achieved. In the

present study, it is observed that the frequency dispersion of the complex dynamic crystal lattice compliance function in the *TD* specimen varies linearly at low temperatures but the variation becomes more remarkable at elevated temperatures corresponding to the temperature range of the α_2 dispersion. This frequency dispersion of dynamic crystal lattice compliance, though still being an apparent parameter as discussed previously[1,18], is believed to associate with the intracrystal relaxation process, thus supporting the above assignment to the α_2 dispersion.

On the other hand, the assignment to the α_1 dispersion corresponding to the lower temperature process of the α mechanical dispersion has being disputed for years. The prevalent assignment was the interlamellar shear or interlamellar grain-boundary process[25-27]. Recently, the assignment of interlamellar shear to the α_1 process has been denied by Takayanagi *et al.* on a bulk-crystallized high-density polyethylene, who separated the α_1 and α_2 processes on the basis of the α_2 relaxation data of single crystal mat. They found that the α_1 process is enhanced upon annealing, i.e. increasing lamellar thickness and consequently decreasing chain folds at the lamellar surface. Their argument was that if the interlamellar shear has to be responsible to the α_1 grain-boundary relaxation, the α_1 process should be reduced with lamellar thickening since the process is proportional to the area of boundary surface. But as their results came out in reverse, they concluded that the α_1 process should not be caused by the interlamellar shear, but rather by an intralamellar shear associated with 'inter-crystal-mosaic-block relaxation' at their boundaries[34-36].

Stachurski and Ward studied on the mechanical dispersions and their anisotropy of oriented polyethylenes. For a low-density polyethylene, they proposed that the α dispersion is activated by the intralamellar *c/c* (*c*-axis/*c*-axis) shear while the β (primary) dispersion is caused by the interlamellar *l/l* (lamella/lamella) shear. Later on, they observed only one α dispersion in an annealed oriented high-density polyethylene with activation energy of the order of 22 kcal mol^{-1}, and assigned it to the interlamellar *l/l* shear. They concluded that the β process of low-density polyethylene and the α process of high-density polyethylene are caused by the same interlamellar *l/l* shear while the α process of low-density polyethylene is activated by the intralamellar *c/c* shear[37-39].

In this study on the row-nucleated high-density polyethylene, two types of distinctive deformation mechanisms contributing to the α_1 dispersion are observed:
(i) lamellar detwisting mechanism involving the rotation of crystal *a*- and *c*-axes around the *b*-axis for the *MD* specimen,
(ii) lamellar shearing mechanism associating with the rotation of the crystal *b*- and *c*-axes around the *a*-axis for the *TD* specimen, as the representatives, respectively, that are expected to occur at the equatorial and polar zones of spherulitic texture.
Both of these dynamic rotation behaviour of the crystallographic axes must be interpreted in terms of the dynamic reorientation of lamellar segments or crystal grains within the lamellae, assigning the α_1 dispersion of these particular specimens as well as the spherulitic specimen to the intralamellar shear.

The former mechanism of lamellar detwisting is not believed to be caused by the rotation of an entire lamellar unit around the lamellar axis, but rather accompanied by localized detwisting of lamellar segments or crystal grains certainly not larger in the size along the lamellar axis than the order of the period of lamellar twisting. This is because the lamellar detwisting, if the lamella is really a single twisted platelet, to have to occur segmentally, not as a whole, so as to align the crystal *c*-axis of the segment parallel to the plane including the lamellar axis and the stretching direction. This type of crystal reorientation within the lamella must be activated by straining of tie-chain molecules between adjacent lamellae in association with a dynamic balance of mechanical consistency (dynamic viscosity) between inter- and intra-lamellar noncrystalline materials. Therefore, the lamellar detwisting mechanism, which is originated from interlamellar shear, is difficult to categorize as either inter- or intra-lamellar shear, depending on the definition of the terminology and, thus, resulting in the disputation.

Nevertheless, we are inclined to distinguish the intra- and inter-lamellar shear in that the interlamellar shear must be limited only for the case of dynamic response of the lamella, as a whole, not associated with any reorientation of the lamellar segments or crystal grains within the lamella. This type of dynamic response may be expected, from the concept of distribution of 'crystal-grain-boundary-relaxation-time' proposed previously[1], as one of the extremes of the balance of dynamic viscosity between the inter- and intra-lamellar noncrystalline materials. As when increasing the frequency of mechanical excitation or decreasing the measuring temperature, the dynamic viscosity of the intralamellar noncrystalline material becomes higher than that of the interlamellar noncrystalline material, so that the lamellae behave like stiff rods within the interlamellar noncrystalline material. This type of dynamic response of the interlamellar shear seems to be significant to assign the β mechanical dispersion of spherulitic crystalline polymers especially in relation to the degree of lamellar twisting.

An additional deformation mechanism of lamellar bending associated with the negative form birefringence is observed for the *MD* specimen in the vicinity of the α dispersion. This lamellar bending occurs in-phase with the dynamic bulk strain, suggesting that the lamellae respond like a leaf-spring to yield the 'hard-elasticity'. The contribution of this process is not found crucial to the α dispersion, but may be significant for the low temperature β dispersion of this material. For a blow-extruded polybutene-1[40], the hard elasticity can disappear, when the temperature is cooled down to the glass transition temperature of this material, and the material exhibits an enormous β dispersion. The hard elasticity of these kinds of row-nucleated materials is not really of elastic nature, but merely an apparent one, at room temperature, hidden from both the α and β relaxation processes.

ACKNOWLEDGEMENTS

This series of rheooptical studies on the deformation mechanisms of semicrystalline polymers is supported in part by a grant from the U.S.-Japan Cooperative Research Program, the National Science Foundation and the Japan Society for Promotion of Science, to which the authors are deeply indebted. The authors are also indebted to the Nippon Gosei Kagaku Co. Ltd., Osada, Japan, and the Dai-Cell Co. Ltd., Osaka, for financial support through a scientific grant.

REFERENCES

1 Suehiro, S., Yamada, T., Inagaki, H., Kyu, T., Nomura, S. and Kawai, H. *J. Polym. Sci. Polym. Phys. Edn.* 1979, **17**, 763
2 Suehiro, S., Kyu, T., Fujita, K. and Kawai, H. *Polym. J.* 1979, **11**, 331
3 Fukui, Y., Sato, T., Ushirokawa, M., Asada, T. and Onogi, S. *J. Polym Sci.* (*A*-2) 1970, **8**, 1195
4 Tanaka, A., Chang, E. P., Delf, B., Kimua, I. and Stein, R. S. *J. Poly. Sci. Poly. Phys. Edn.* 1973, **11**, 1891
5 Stein, R. S., Finkelstein, R. S., Yoon, D. Y. and Chang, C. *J. Polym. Sci.* (*C*) 1974, **46**, 15
6 Kyu, T., Yasuda, N., Suehiro, S., Nomura, S. and Kawai, H. *Poly. J.* 1976, **8**, 565
7 Wang, T. T. *J. Polym. Sci. Polym. Phys. Edn.* 1974, **12**, 145
8 Hashimoto, T., Prud'homme, R. E. and Stein, R. S. *J. Polym. Sci. Polym. Phys. Edn.* 1973, **11**, 709
9 Sasaguri, K., Yamada, R. and Stein, R. S. *J. Appl. Phys.* 1964, **35**, 3188
10 Oda, T., Nomura, S. and Kawai, H. *J. Polym. Sci.* (*A*) 1965, **3**, 1993
11 Oda, T., Sakaguchi, N. and Kawai, H. *J. Polym. Sci.* (*C*) 1966, **15**, 223
12 Nomura, S., Asanuma, A., Suehiro, S. and Kawai, H. *J. Polym. Sci.* (*A*-2) 1971, **9**, 1991
13 Nomura, S., Matsuo, M. and Kawai, H. *J. Polym. Sci. Polym. Phys. Edn.* 1972, **10**, 2489
14 Nomura, S., Matsuo, M. and Kawai, H. *J. Polym. Sci. Poly. Phys. Edn.* 1974, **12**, 1371
15 Yoon, D. Y., Chang, C. and Stein, R. S. *J. Polym. Sci. Polym. Phys. Edn.* 1974, **12**, 2091
16 Matsuo, M., Hattori, H., Nomura, S. and Kawai, H. *J. Polym. Sci. Polym. Phys. Edn.* 1976, **14**, 233
17 Hashimoto, T., Nagatoshi, K., Todo, A. and Kawai, H. *Polymer* (*London*), 1976, **17**, 1063
18 Suehiro, S., Yamada, T., Kyu, T., Fujita, K., Hashimoto, T. and Kawai, H. *Polym. Eng. Sci.* 1979, **19**, 929
19 Kyu, T., Yasuda, N., Tabushi, M., Nomura, S. and Kawai, H. *Poly. J.* 1975, **7**, 108
20 Keller, A. and Machin, M. J. *J. Macromol. Sci.* (*B*) 1967, **1**, 41
21 Quynn, R. G. and Broady, H. *J.* Macromol. Sci. (B) 1971, **5**, 721
22 Sprague, B. S. *J. Macromol. Sci.* (*B*) 1973, **8**, 157
23 Clark, E. S. 'Structure and Properties of Polymer Films', (Eds. R. W. Lentz and R. S. Stein) Plenum Press, New York, 1973, p 267
24 Nakayasu, H., Markovitz, H. and Plazek, D. J. *Trans. Soc. Rheol.* 1961, **5**, 261
25 Iwayanagi, S. and Nakane, H. *Rept. Prog. Polym. Phys. Japan*, 1964, **7**, 179
26 McCrum, N. G. and Morris, E. L. *Proc. Roy. Soc.* (*London*), 1966, **A292**, 506
27 Hideshima, T. and Kakizaki, M. *J. Macromol. Sci.* (*B*) 1973, **8**, 368
28 Hoffman, J. D., Williams, G. and Passaglia, E. *J. Polym. Sci.*, (*C*) 1966, **14**, 173
29 Hayakawa, R. and Wada, Y. *Rept. Prog. Polym. Phys. Japan.* 1966, **9**, 193; 1968, **11**, 215
30 Peterlin, A. and Fischer, E. W. *Z. Phys.* 1960, **159**, 272; *J. Chem. Phys.* 1962, **37**, 1403
31 Suehiro, S., Yamada, T., Inagaki, H. and Kawai, H. *Poly. J.* 1978, **10**, 315
32 Stein, R. S., Kawaguchi, T., Kimura, I. and Takeuchi, A. *J. Polym. Sci.* (*B*) 1967, **5**, 339
33 Bunn, C. W. and Daubeny, R. *Trans. Faraday Soc.* 1954, **50**, 1173
34 Kajiyama, T., Okada, T., Sakoda, A., and Takayanagi, M. *J. Macromol. Sci.* (*B*) 1973, **7**, 583
35 Kajiyama, T., Okada, T., and Takayanagi, M. *J. Macromol. Sci.* (*B*) 1974, **9**, 35
36 Takayanagi, M. *J. Macromol. Sci. Phys.* 1974, **B9(3)**, 391
37 Stachurski, Z. H. and Ward, I. M. *J. Polym. Sci. A*-2 1968, **6**, 1083
38 Stachurski, Z. H. and Ward, I. M. *J. Poly. Sci. A*-2 1968, **6**, 1817
39 Stachurski, Z. H. and Ward, I. M. *J. Macromol. Sci.* (*B*) 1969, **3**, 445
40 Hashimoto, T., Todo, A., Tsukahara, Y. and Kawai, H. *Polymer* (*London*) 1979, **20**, 636